Low Temperature Physics/Fizika Nizkikh Temperatur, 2020, vol. 46, No. 11, pp. 1310–1317

Effect of doping level and compensation on thermal conductivity in $Ce_xSn_{1-x}Se$ solid solutions

Sh. S. Ismailov

Institute of Radiation Problems of Azerbaijan National Academy of Sciences, Baku, Azerbaijan

J. I. Huseynov

Azerbaijan State Pedagogical University, Baku, Azerbaijan

M. A. Musaev and I. I. Abbasov

Azerbaijan State Oil and Industry University, Baku, Azerbaijan
E-mail: ibrahimabbasov179@gmail.com

V. A. Abdurakhmanova

Institute of Physics of Azerbaijan National Academy of Sciences, Baku, Azerbaijan

Received March 28, 2020, revised August 10, 2020, published online September 21, 2020

The paper reports the results of experimental studies of the thermal conductivity and density of $Ce_xSn_{1-x}Se$ solid solutions in the temperature range 80–480 K. Under the assumption of elastic scattering of charge carriers, parabolic band and arbitrary degeneracy, the electronic and lattice components of thermal conductivity have been calculated. The characteristic features of the thermal conductivity of these crystals have been analyzed, it has been shown that with an increase in cerium content and with an increase in temperature, the total (χ_{tot}) and lattice (χ_{ph}) thermal conductivity significantly decrease, while the density increases slightly (at 300 K). The dependence of thermal conductivity on the percentage of cerium in the composition has been established. With prolonged annealing, the total and lattice components of thermal conductivity increase. It has been established that heat transfer in $Ce_xSn_{1-x}Se$ is carried out mainly by phonons.

Keywords: solid solutions, lattice thermal conductivity, thermal resistance, point defects, phonon-phonon scattering.

1. Introduction

The thermoelectric properties of traditional materials have been significantly improved over the past decades. Graphene, black phosphorus, transition metal dichalcogenides, $A^{IV}B^{VI}$ compounds, and other layered two-dimensional (2D) materials are in the focus of attention of the researchers as high-potential thermoelectric materials. Numerous $A^{IV}B^{VI}$-based semiconductor solid solutions have been explored in greater detail and have found their application in the development of various energy converters [1–3]. Recently, tin selenide (SnSe) and solid solutions based on it have been intensively studied in various research centers [4–7]. The excellent thermoelectric characteristics of SnSe are attributed to its ultra-low lattice thermal conductivity. SnSe has layered structures and causes anisotropic thermoelectric properties along different crystallographic axes, however, they have not yet found practical application in serial devices, since the thermoelectric efficiency relative to other $A^{IV}B^{VI}$ group of compounds is low ($Z \approx (0.8-2.4)\cdot 10^{-3}\,K^{-1}$) [6, 7]. In SnSe, the bandgap — $E_g \approx 0.9$ eV, the electrical conductivity ($\sigma \approx 14-68\ \Omega^{-1}\cdot cm^{-1}$) and the thermal conductivity $\chi \approx (16.8-18.7)\cdot 10^{-3}$ W/(cm·K) are small, the thermal EMF varies $S \approx 380-600\ \mu V/K$ and is prone to optical properties [9, 10]. That is, it is in an intermediate state between thermoelectric and optical materials.

In [4], the crystal structure, thermal conductivity, heat capacity, and thermal expansion of SnSe have been studied in wide temperature ranges. Debye temperatures have been determined and the presence of two characteristic vibrational energy scales in SnSe with temperatures $\theta_{D_1} = 345(9)$ K and $\theta_{D_2} = 154(2)$ K have been noted, which have been associated with strong (in layers) and weak (between layers) chemical bonds Sn–Se.

Thermoelectric and galvanomagnetic properties and density in doped materials have been studied: 1.0 % Ag and 1.0; 2.0 % Na. It has been revealed that the concentration of charge carriers (n) increases from $0.42\cdot10^{18}$ to $51.8\cdot10^{18}$ cm^{-3}, the mobility decreases from 138.4 to 84.4 $cm^2/(V\cdot s)$, respectively. The density of SnSe and the compositions of the doped samples, as well as the thermoelectric parameters, have been determined, in which the thermoelectric figure of merit changes: $ZT = 0.03 - 0.22$, respectively. The density of a binary SnSe compound has been studied by several authors [4, 6, 8]. The difference between the experimental data can be caused by the difference in the characteristics of the sample arising from sample preparation and processing methods or measurement errors. Despite these or other technological imperfections, the thermal conductivity is low [at 300 K $\chi = 1.78$ W / (m · K)] and the density fluctuates in the range $6.0 - 6.2$ g / cm^3.

In [4, 6], it has been indicated that the density does not strongly affect the thermal conductivity of the sample, and especially the lattice thermal conductivity. SnSe samples obtained by the Bridgman method deviate from the stoichiometric composition and crystallize with Sn vacancies. The authors of [6] have measured the density of SnSe in several ways and compared it with theoretical calculations, including x-ray diffraction studies, and obtained $6.13 - 6.18$ g / $см^3$. They have determined that SnSe has an ultra-low electrical conductivity equal to $\sigma \cong 2.3 - 14\ \Omega^{-1}\cdot cm^{-1}$.

Impurities in SnSe behave in a very peculiar way: Sb behaves as a donor at a temperature up to 200 °C and as an acceptor at higher temperatures [11]. This is possible if at low temperatures Sb atoms replace Sn atoms in the SnSe lattice, and at high temperatures, Se atoms. The authors of [12, 13] have studied SnSe and $A^{III}Se$(A^{III} –Ga, In, Tl, As) and found that $SnSe - A^{III}Se$ solid solutions are promising materials for creating photoelectric and thermoelectric converters, especially with an admixture of thallium for creating thermoelectric generators and photoresistors.

In recent years, solid solutions with the participation of rare earth elements (REE) [9, 14–17] have been intensively studied for solving various scientific and technical problems. The development of technology for their production in the form of good crystals or films leads to a significant expansion of the practical application of these materials. Various thermoelectric converters are manufactured with the participation of trivalent REE, including La, Ce, Pr, Er, Nd, etc.

The introduction of REE chalcogenides leads to a number of physical features due to the complex nature of defect formation and the interaction of defects. Interest in p-SnSe involving cerium is mainly due to the peculiarities of the possibility to obtain new photovoltaic and thermoelectric materials operating at relatively high temperatures (T = = 300 – 900 K). In the present paper, as a continuation of [14], the thermal conductivity of single crystals of $Ce_xSn_{1-x}Se$ solid solutions has been investigated in the temperature range 80–480 K.

2. Experimental technique

The samples have been prepared by fusing the initial components in evacuated (p = 0.1 Pa) quartz ampoules at a temperature of 1000 °C for 6 h. The initial components were: tin of grade B4-000; selenium OS417-4 and chemically pure elemental cerium CEE-0 with a purity of 99,95 %.

After synthesis single crystals have been grown by the Bridgman–Stockbarger method. The synthesized samples for investigation of the physical and thermal properties have been annealed for 140–210 h depending on the composition: the annealing time was increased with increasing cerium content — by the slow cooling method with a constant temperature gradient along the ingot. Homogenizing annealing of the obtained chemically single-phase samples has been carried out in the medium of spectrally pure argon at 800 K [15]. Given that the samples have only structural defects, annealing has been carried out with slow heating at a rate of 250 K / h and cooled down to room temperature at a rate of $v_{cool} = 150$ K / h. The compositions of the synthesized samples has responded to the values $x = 0$ (No. 1); $x = 0.005$ (No. 2); $x = 0.01$ (No. 3); $x = 0.015$ (No. 4); $x = 0.02$ (No. 5) and $x = 0.025$ (No. 6) at. % Ce (sample numbers correspond to alloy compositions).

The interaction in the SnSe–CeSe system has been studied by differential thermal (DTA), x-ray diffraction (XRD), microstructural (MSA) analyzes, as well as microhardness measurement and density determination [14]. The structure, phase and elemental composition of the obtained ingots and the surface state along the plane of the natural layers of the samples under study has been determined by conducting complex x-ray diffraction, radiographic, x-ray spectroscopy, and microscopic analyzes. X-ray diffraction analysis has been performed with a MiniFlex x-ray diffractometer (Rigaku Corporation) at 30 kV, 10 mA, CuK_α radiation ($\lambda = 1.5406$ Å). Diffraction reflections have been observed at a step size of 0.01° and a bias angle of 2θ in the range 0–80°.

To investigate the morphology and microstructure of the sample surface, the Japanese-made scanning electron microscope (SEM) JEOL JSM6610-LV has been used. In the study of the surface relief, the semicontact method has been applied, which is the basis for the implementation of a number of other methods associated with the use of resonant frequency of the cantilever. An NSG10 silicon cantilever has been used at an operating frequency of 280 kHz. Since there was little information on the surface properties of the samples under study, the scanning has been started from a region measuring 10 – 15 μm. Based on the results of scanning this area the optimal values of the scanning speed has been selected and set, then the scanning area has been changed. Surfaces with a smooth relief have been scanned at a higher speed than surfaces with a more developed relief with significant differences in height.

The studied samples also had *p*- and *n*-type conductivity depending on the content of cerium (Ce) impurities. Samples of $\sim 16\times 2\times 4(4.5)$ mm in size have been cut from crystal ingots on an electrospark installation. When cutting, we took into account the layered structure of the compositions and tried not to damage the samples. The thermal conductivity has been measured by the absolute stationary method according to the procedure described in [18, 19], in the crystal growth direction, i. e., along a [110] direction. The error in the measurement of thermal conductivity was less than 6 %.

A vacuum of about 0.1 Pa has been created in the cryostat, the temperature has been determined by a copper-constant thermocouple having a cross section of ⦰ 0.12 mm. Along the sample had a temperature gradient $\Delta T = 6 - 10$ K. The distance between the gradient probes was $\Delta L = 6$ mm. The measuring circuit used: power supply TES-41, universal voltmeter V7-21 and V7-21A, potentiometer R4833, ammeters Ts4311.

The thermal conductivity of the samples has been determined by the formula [18, 19]

$$\chi = \frac{w-\Sigma}{\Delta L}\frac{S}{l}\left(\frac{\mathrm{W}}{\mathrm{cm}\cdot\mathrm{K}}\right),$$

where w is the power of the gradient furnace ($w = JU$), $\Sigma = Q_{\mathrm{rad}} - Q_w$ is the total heat loss, S is the section of the sample, l is the sample length, ΔL is the distance between probes, Q_{rad} is the radiation loss, Q_w is the heat loss from wires.

3. Results and discussion

The results of comprehensive physicochemical analyzes show that the $Ce_xSn_{1-x}Se$ alloy system, like the base SnSe substance, crystallizes into a distorted sodium chloride structure with a strong intralayer and weak (Van der Waals type) interlayer interaction, closely related to the structure of black phosphorus, has an orthorhombic crystal lattice structure with the space group P_{nma}. The structure consists of tightly bound double layers and can be considered as a distorted rock salt phase. At atmospheric pressure the crystal structure is layered. These compounds exhibit properties intermediate between two-dimensional layered systems and three-dimensional crystals.

With an increase in the percentage of CeSe in the composition, a slight increase in the unit cell parameters of the crystal lattice, density and microhardness is observed, and heat effects are shifted to the region of relatively lower temperatures. The observed increase in lattice parameters, good agreement between the partial replacement of Sn atoms by Ce atoms of a larger radius and compliance of Vegard's law suggests the formation of substitutional solid solutions based on SnSe.

The composition of the phase and the distribution of chemical elements on the surface of the sample under study have been determined by quantitative x-ray microanalysis. An analysis of the results shows surface homogeneity, but with a change in stoichiometry within the SnSe homogeneity region towards excess selenium.

In spite of the fact that SnSe single crystals are layered crystals, some roughness is observed on the natural cleaved surface. Sometimes, during cleavage, mechanical influences can break interatomic bonds in the structure along planes located from the surface at a distance of several atomic layers. The resulting mechanical stresses in the thin atomic grid lead to the formation of folded surfaces.

Figure 1 represents an SEM image of the surface of SnSe and $Ce_{0.01}Sn_{0.99}Se$ crystals obtained by cleavage and subjected to mechanical stress, a fragment of this surface is given together with a profilogram. The observation of certain roughness in the boundary layer is likely related to the presence of weak Van der Waals forces between the layers, moreover, when the bonding forces are destroyed, not individual atoms remain on the crystal surface, but entire groups of atoms — clusters. In the binary compound SnSe the partial replacement of Sn atoms by rare-earth metal atoms of even larger radius enhances the weak Van der Waals bond between the layers. Thus, with an increase in the amount of Ce in the composition of the $Ce_xSn_{1-x}Se$ alloy system, layer-by-layer rejection becomes more complicated and the roughness of the natural surface increases. The resulting mechanical stress in the thin atomic grid leads to the formation of folded surfaces shown in Figs. 1(a) and (b). A histogram analysis of the obtained SEM images and a surface profilogram show that the natural surface homogeneity of the SnSe single crystal varies within 15 nm. As the amount of Ce in the composition of the $Ce_xSn_{1-x}Se$ single crystal increases, the inhomogeneity and surface roughness also increases [Figs. 1(b), (d)].

Research findings of the temperature dependence of the total thermal conductivity of unannealed and annealed samples of $Ce_xSn_{1-x}Se$ solid solutions are shown in Fig. 2. As can be seen in Fig. 2, with increasing temperature, the total thermal conductivity (χ_{tot}) in the studied temperature range decreases. Annealing leads to a certain increase in thermal conductivity (by 12–20 %) for all samples, while the nature of the temperature dependence does not change [15, 17].

As can be seen, in the temperature range 80–360 K the coefficient of total thermal conductivity (χ_{tot}) changes according to normal phonon heat transfer processes. With the increase in the cerium content in $Ce_xSn_{1-x}Se$ solid solutions, the value of χ_{tot} decreases. The exception is sample No. 6, with *n*-type conductivity, in which the total thermal conductivity increases in the region $T > 350$ K with increasing temperature (Fig. 2, curve *6*).

The process of heat transfer in semiconductors, generally, is carried out by vibrations of the crystal lattice, electron gas, electromagnetic radiation, bipolar diffusion of charge carriers:

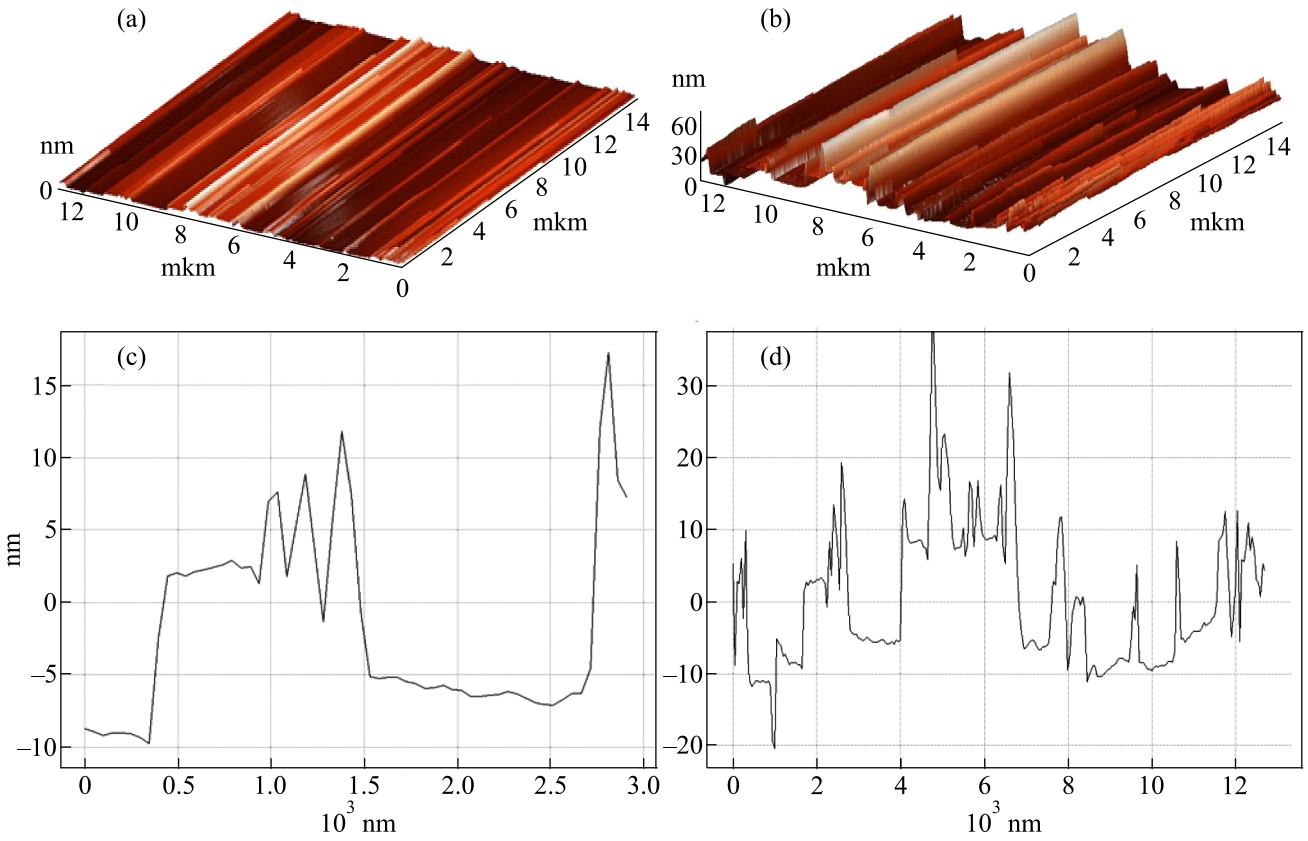

Fig. 1. SEM images of SnSe (a), (c) and $Ce_{0.01}Sn_{0.99}Se$ (b), (d) crystal surfaces obtained with fresh cleavages and subjected to mechanical stress: (a), (b) — folding of surfaces; (c), (d) — surface profilograms.

$$\chi_{tot} = \chi_{ph} + \chi_{el} + \chi_{phot} + \chi_{bp}, \qquad (1)$$

where χ_{ph}, χ_{el}, χ_{phot}, χ_{bp} are the lattice, electronic, photonic and bipolar components of thermal conductivity. The contribution of each term is largely determined by the electronic structure of the substance and temperature. For instance, photonic thermal conductivity plays an important role at high temperatures, especially for transparent bodies, and, conversely, is insignificant at low temperatures. Given that the absorption coefficient of tin selenide is rather high $\alpha \sim 200\ cm^{-1}$, the photonic component of thermal conductivity can be neglected. Since the intrinsic conductivity in SnSe occurs at temperatures above room temperature (550–600 K), we believe that in the temperature range up to 500 K, bipolar diffusion of charge carriers does not occur. Accordingly, the total thermal conductivity is determined by the lattice (phonon) and electronic components [15, 17].

To elucidate the mechanism of the influence of annealing and cerium content on the thermal conductivity of $Ce_xSn_{1-x}Se$, the electronic (χ_{el}) and lattice (χ_{ph}) components of the thermal conductivity were calculated. Using the Wiedemann–Franz law, the fractions of electronic thermal conductivity (χ_{el}) are calculated, and then using the difference ($\chi_{tot} - \chi_{el}$) the values of χ_{ph} are found. When calculating the electronic component of thermal conductivity, the experimentally obtained values of the coefficients of thermoEMF (S) and electrical conductivity (σ) of the samples have been used [14, 16]. Calculations have been performed according to the method described in [20, 21].

If there is a contribution to the total thermal conductivity only the lattice (χ_{ph}) and electronic (χ_{el}) components then the total thermal conductivity of the material is determined by the sum of these quantities:

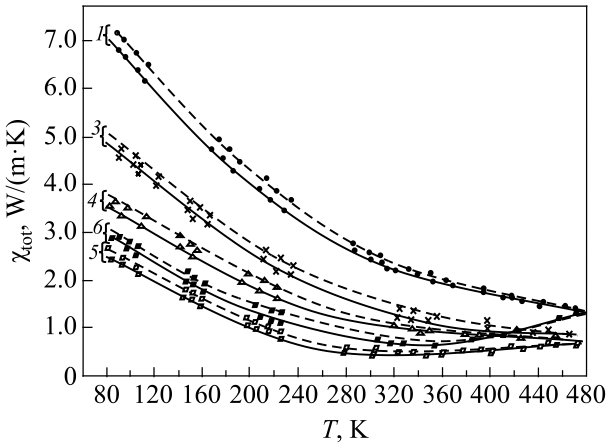

Fig. 2. Temperature dependences of the coefficient of total thermal conductivity of $Ce_xSn_{1-x}Se$ solid solutions before (solid lines) and after (dotted lines) annealing in the compositions $x_1 = 0$ (*1*); 0.01 (*3*); 0.015 (*4*); 0.020 (*5*); 0.025 (*6*).

$$\chi_{tot} = \chi_{ph} + \chi_{el}. \quad (2)$$

Having calculated χ_{el} on the basis of experimental data, lattice thermal conductivity has been determined from (2).

The electronic component of thermal conductivity for the parabolic zone in the case of arbitrary degeneracy and elastic scattering of charge carriers was calculated by the formula

$$\chi_{el} = L\sigma T, \quad (3)$$

where $L = A(k/e)^2$ is the Lorentz number. The calculations assumed that the scattering of charge carriers occurs on the acoustic lattice vibrations. The value of A has been determined from the dependence $A = f(\sigma)$ [4, 21].

The value of the Lorentz number L (in our calculations) for SnSe is $1.03\cdot10^{-8}$ $(V/K)^2$ and the total thermal conductivity χ_{tot} for SnSe is in satisfactory agreement with the data [21].

The temperature dependences of the lattice thermal conductivity coefficient for SnSe and $Ce_xSn_{1-x}Se$ solid solutions are shown in Fig. 3. The results reveal that with increasing cerium content in $Ce_xSn_{1-x}Se$ solid solutions, the values χ_{ph} decrease. In this regard annealing leads to an increase in both χ_{tot} and χ_{ph} of the samples (Fig. 2, dotted lines).

The Figs. 2 and 3 show that, depending on the content of cerium impurities, the total and lattice thermal conductivity decrease. At the same time, as the temperature increases, χ_{tot} and χ_{ph}, respectively, decrease.

The power-law index of thermal conductivity was estimated, which was determined from the temperature dependences of χ in the temperature range 80–400 K, according to the formula $\chi \sim T^{-n}$, here T is the temperature, n is the power-law index. For tin selenide ($x = 0$), the thermal conductivity to temperatures of 400 K decreases according to the law $\chi \sim T^{-0.9}$ and is mainly determined by the phonon component. When the concentration of cerium in $Ce_xSn_{1-x}Se$ solid solutions increases, n decreases. We associate a decrease in the power-law index in $Ce_xSn_{1-x}Se$ solid solutions with the appearance of additional phonon scattering centers with an increase in the concentration of the dopant. It is conceivable that the deviation of $\chi(T)$ from the law T^{-1} is associated with the influence on the heat transfer mechanism of both the electronic component of thermal conductivity and a change in the defect structure [9, 15].

Further, from the temperature dependence of χ_{ph}, the values of the thermal resistance of the crystal lattice $w = 1/\chi_{ph}$ were calculated, which allowed us more clearly analyze the mechanism of heat transfer in $Ce_xSn_{1-x}Se$ solid solutions. The temperature dependences of the thermal resistance of the lattice before and after annealing for all samples in the range 80–340 K are linear (Fig. 4), indicating that thermal resistance is created by phonon-phonon scattering and an increase in w in $Ce_xSn_{1-x}Se$ with an increase in x (Ce concentration) is caused by phonon scattering by point (vacant) defects (Fig. 4, solid lines are shown only for three samples: Nos. 1, 3, 6).

Given that unannealed samples differ from annealed ones only with the presence of structural defects, it can be suggested that the following relation is valid:

$$\frac{1}{\chi'_{ph}} = \frac{1}{\chi_{ph}} + \frac{1}{\chi_D}, \quad (4)$$

where χ'_{ph} and χ_{ph} are the thermal conductivity of unannealed and annealed samples at 800 K, from which the value $1/\chi_D$ that characterizes the additional phonon scattering by defects is calculated. The concentration of defects in unannealed samples is found using the formula in [9, 20]:

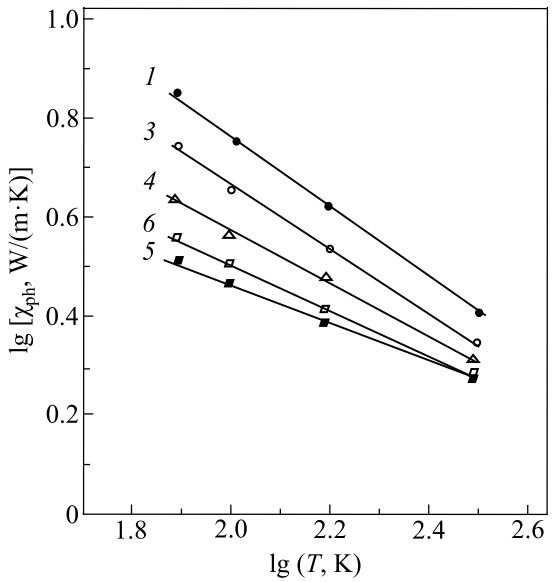

Fig. 3. Temperature dependences of lattice thermal conductivity in the $Ce_xSn_{1-x}Se$ system: $x = 0$ (*1*); 0.01 (*3*); 0.015 (*4*); 0.02 (*5*); 0.025 (*6*).

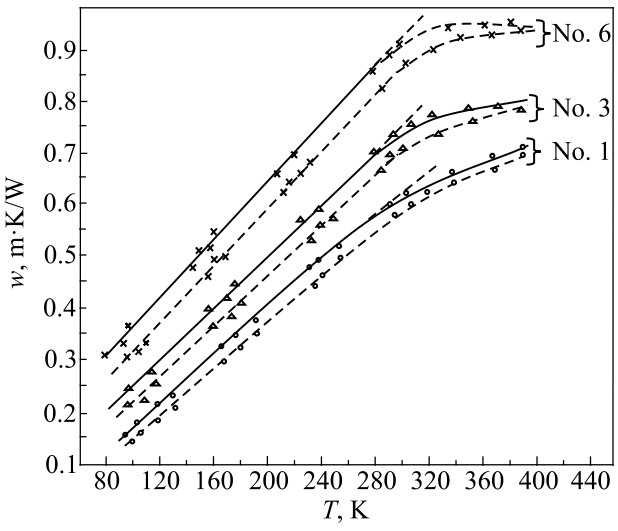

Fig. 4. Temperature dependences of thermal resistance of $Ce_xSn_{1-x}Se$ crystals: before (solid lines) and after (dotted lines) annealing in compositions: $x = 0$ (No. 1); 0.01 (No. 3); 0.025 (No. 6).

$$\chi_{el} = \frac{0.9hv^2G^{-1}}{12\pi^2TV_0S^2}, \quad (5)$$

where V_0 is the volume of the unit cell, v is the speed of sound, G^{-1} is the number of defects in the unit cell of the sample, S is the scattering parameter (usually taken to be unity) [21], T is the absolute temperature.

$Ce_xSn_{1-x}Se$ solid solutions crystallize in the deformed NaCl-type structure. For a slightly deformed cubic lattice at 80 K, the lattice constants for the samples studied are $a = 4.33$ Å, 4.35 Å, 4.36 Å, and 4.38 Å at $x = 0$, 0.01, 0.015, 0.025, respectively [14]. Based on these data, the volume of the unit cell V_0 has been calculated. The speed of sound in the samples was determined from the ratio

$$v = \sqrt{\frac{E}{\rho}}, \quad (6)$$

where $E = 10.8 \cdot 10^8$ Pa is a Young's modulus, $\rho = 6.28 \cdot 10^3$ kg / m^3 [14, 16].

The calculation results are shown in Fig. 5, which show the dependence of lattice thermal conductivity χ_{ph} on the concentration of defects, both structural [15, 21] and those caused by cerium atoms. The total concentration of charge carriers depending on the cerium content in $Ce_xSn_{1-x}Se$ is also shown. As Fig. 5(a) demonstrates, at $x \approx 0.02$ at. % Ce, the sign of the charge carrier conductivity changes from *p*- to *n*-type. Closer to this composition, the lattice thermal conductivity (χ_{ph}) before [Fig. 5(b), solid lines] and after annealing [Fig. 5(b), dotted lines] take a minimum value. With a further increase in the cerium content in $Ce_xSn_{1-x}Se$, the composition has *n*-type conductivity (sample No. 6 [14]). Apparently, this is due to the process of incorporation of cerium atoms into Sn vacancies under the condition of electroneutrality of the composition $n = [L^*_{Sn}]$. For hole concentration, the expression $p = K_i[L^*_{Sn}]^{-1}$ is obtained, that is, the hole concentration decreases as the tin vacancy is replaced, which is observed in Fig. 5. That is, the intrinsic concentration constant K_i for $Ce_xSn_{1-x}Se$ is proportional to the square of cerium ionization at the tin nodes [14, 16].

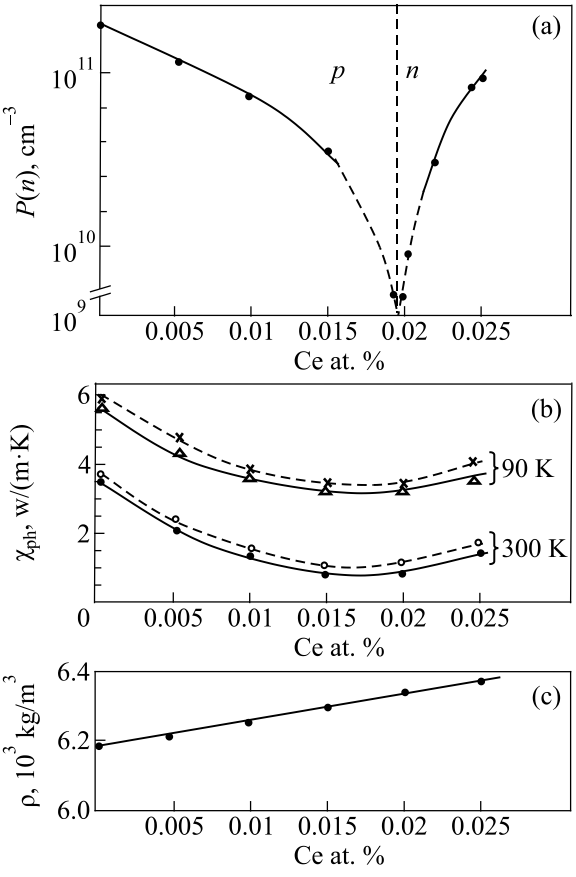

Fig. 5. Dependence of the concentration of charge carriers (a); lattice thermal conductivity (b): before (solid lines) and after (dotted lines) annealing, and density (c) on the content of cerium impurities in $Ce_xSn_{1-x}Se$ solid solutions at $T = 300$ K.

Calculations show that with an increase in the cerium content, the concentration of defects (vacancies) decreases, and the density slightly increases [14]. In contrast, the scattering centers also increase accordingly (i. e., the anharmonicity increases). Therefore, cerium metal, on the one hand, partially "purifies" crystals from point defects, on the other hand, gives rise to additional scattering centers, and these two opposite influences play the main role in the perfection of crystals. As can be seen from the graph [Fig. 5(b), dotted lines] in the annealed samples the lattice thermal conductivity is much improved due to the reduction of structural defects. However, as the concentration of Ce increases, local distortion of the crystal lattices occurs. The introduction of the Ce impurity into the crystal leads to a disruption of the crystal potential, which is consistent with a significant difference in the chemical sizes of Sn^{2+} and Ce^{3+} ions in the crystal ($r_{Sn} = 0.94$ Å, $r_{Ce} = 1.18$ Å). In turn, annealing leads to ordering of the crystal structure (healing of structural defects), as a result of which the thermal conductivity of the samples increases (Figs. 2 and 4) [15, 17].

In the samples under study, the impurities are compensated by intrinsic defects, and with an increase in the Ce content, a change in the sign of *p*- to *n*-type of conductivity is observed. It is established that for crystalline $Ce_xSn_{1-x}Se$ samples, the lattice thermal conductivity plays the main role. The electronic fraction of thermal conductivity for unannealed samples at 80 K is less than 1 % of the total thermal conductivity for SnSe, and for solid solutions from 0.36 to 1.2 % (in sample No. 6). After annealing at 800 K, the electronic component of the thermal conductivity of the samples with Ce increases to 8 % at $T < 320$ K.

The electrophysical properties of some $Ce_xSn_{1-x}Se$ compositions have been previously studied in [14]. The parameter results have been illustrated in Table 1. The table clearly shows that with an increase in the cerium content, the concentration of holes decreases and, accordingly, the conductivity (σ) and thermoEMF (S) decrease and in the composition $x = 0.02$ the sign of the conductivity *p* changes to *n*-type, which is consistent with the results in Fig. 5(a).

Table 1. The parameters of some $Ce_xSn_{1-x}Se$ compositions

Compositions of $Ce_xSn_{1-x}Se$	ρ, m^{-3}	S, μV/K	σ, 10^{-2} $(\Omega\cdot m)^{-1}$	μ, $cm^2/(V\cdot s)$	χ_{tot}, 10^{-3} W/(cm·K)
$x = 0$	$8.9\cdot10^{23}$	430	64.05	160	18.7
$x = 0.005$	$1.1\cdot10^{23}$	320	26.05	52	
$x = 0.01$	$3.5\cdot10^{22}$	340	14.20	49	
$x = 0.015$	$3.1\cdot10^{22}$	310	8.12	26	
$x = 0.02$	$5.2\cdot10^{21}$	–172	92.36	284.4	

Figure 5 (b) shows that the lattice thermal conductivity (k_{ph}) in the composition decreases with an increase in the cerium content: in sample No. 2 ($x = 0.005$) by 13 %, in sample No. 5 ($x = 0.02$) by 33,3 % and in sample No. 6 ($x = 0.025$) by 29.2 %. Heat treatment of the samples significantly affects the lattice thermal conductivity (dotted line — after annealing). The density of the samples, depending on the Ce impurity content, varies from 6180 kg/m^3 (for SnSe) to 6380 kg/m^3 [Fig. 5(c)].

Conclusion

The electronic and lattice components of thermal conductivity have been calculated and it has been shown that the heat transfer in these materials is mainly carried out by phonons. With an increase in the Ce concentration, a decrease in the power-law index n has been observed in the temperature dependence of the thermal conductivity ($\chi \propto T^{-n}$), due to the appearance of additional centers of phonon scattering with an increase in the concentration of the dopant. It has been established that thermal resistance is created due to phonon-phonon scattering and the increase in thermal resistance with an increase in cerium content is due to the scattering of phonons by point defects. With an increase in the Ce content in solid solutions, partial "purification" occurs and this in turn leads to a slight increase in density and a decrease in thermal conductivity. Prolonged annealing leads to the ordering of the crystal structure, as a result of which the thermal conductivity of the samples increases.

1. S. Roychowdhury, M. Samanta, S. Perumal, and K. Biswas, *Chem. Mater.* **30**, **17**, 5799 (2018).
2. W. Shi, M. Gao, J. Wei, J. Gao, E. Ashalley, H. Li, and Z. Wang, *Adv. Sci.* **5**, 1700602 (2018).
3. *Lead Chalcogenides: Physics and Applications* [ser. Optoelectronic Properties of Semiconductors and Superlattices, v. 18], D. Khokhlov (ed.), N.Y.–London, Taylor and Francis (2003), p. 385.
4. S. R. Popuri, M. Pollet, R. Decourt, M. L. Viciu, and J. W. G. Bos, *Appl. Phys. Lett.* **110** (25), 253903 (2017).
5. S. Li, Z. Tong, and H. Bao, *J. Appl. Phys.* **126** (2), 025111 (2019).
6. S. Wang, S. Hui, K. Peng, T. P. Bailey, W. Liu, Y. Yan, X. Zhou, X. Tang, and C. Uher, *Appl. Phys. Lett.* **112**, 142102 (2018).
7. M. R. Burton, S. Mehraban, D. Beynon, J. McGettrick, T. Watson, N. P. Lavery, and M. J. Carnie, *Adv. Energy Mater.* **9**, 1900201 (2019).
8. P.-C. Wei, S. Bhattacharya, J. He, S. Neeleshwar, R. Podila, Y. Y. Chen, and A. M. Rao, *Nature* **539** (7627), E1–E2 (2016).
9. J. I. Huseynov, M. I. Murquzov, R. F. Mamedova, and Sh. S. Ismailov, *Thermal Conductivity and Termal EMF of Materials for Thermal Energy Converters*, in: TPE-06 3rd Intern. Conf. on Technical and Physical Problems in Power Engineering, Ankara (2006), p. 804.
10. C. Zhang, H. Ouyang, R. Miao, Y. Sui, H. Hao, Y. Tang, J. You, X. Zheng, Z. Xu, X. Cheng, and T. Jiang, *Adv. Opt. Mater.* **7**, 1900631 (2019).
11. S. Patel, S. H. Chaki, and P. C. Vinodkumar, *J. Cryst. Growth* **522**, 16 (2019).
12. V. Kucek, T. Plechacek, P. Janicek, P. Ruleova, L. Benes, J. Navratil, and C. Drasar, *J. Electr. Mater.* **45**, 29439 (2016).
13. Q. Wang, W. Yu, X. Fu, C. Qiao, C. Xia, and Y. Jia, *Phys. Chem. Chem. Phys.* **18**, 8158 (2016).
14. I. I. Abbasov, Sh. S. Ismailov, J. I. Huseynov, and V. A. Abdurahmanova, *Fiz. Nizk. Temp.* **45**, 1509 (2019) [*Low Temp. Phys.* **45**, 1277 (2019)].
15. D. I. Huseynov, M. I. Murguzov, and Sh. S. Ismailov, *Inorganic Mater.* **44**, No. 4, 1 (2008).
16. Sh. S. Ismailov, R. I. Selm-zade, V. A. Abdurakhmanova, and A. A. Sadigova, *Inversion of the Conductivity Type and Thermoelectromotive Force in Solid Solutions $Ce_xSn_{1-x}Se$*, in: Materials of the XI International Scientific and Technical Conference Micro- and Nanotechnology in Electronics, Nalchik, 2019, p. 94.
17. J. I. Huseynov and T. A. Jafarov, *World J. Condens. Matter Phys.* **4**, No. 1 (2014).
18. A. S. Okhotin, A. S. Pushkarsky, R. P. Borovikova, and V. A. Simonov, *Methods for Measuring Characteristics of Thermoelectric Materials and Converters*, Moscow, Nauka (1974) (in Russian).
19. Yu. I. Stern, *Methods for Studying the Thermal and Electrophysical Properties of Materials*, in: Factory Laboratory. Diagnostics of Materials **74**, No. 6, 32 (2008) (in Russian).
20. J. Drable and G. Goldsmith, *Thermal Conductivity of Semiconductors*, Foreign Literature Publishing House, Moscow (1963) (in Russian).
21. I. A. Smirnov and V. I. Tamarchenko, *Electronic Thermal Conductivity in Metals and Semiconductors*, Nauka, Leningrad (1977) (in Russian).

Вплив рівня допіювання та компенсування на теплопровідність твердих розчинів $Ce_xSn_{1-x}Se$

Sh. S. Ismailov, J. I. Huseynov, M. A. Musaev, I. I. Abbasov, V. A. Abdurakhmanova

Представлено результати експериментальних досліджень теплопровідності та густини твердих розчинів Ce_xSn_{1-x} Se в інтервалі температур 80–480 К. В припущенні пружного розсіювання носіїв заряду, параболічної зони та довільного виродження розраховано електронну й ґраткову складові теплопровідності. Проаналізовано характерні особливості теплопровідності цих кристалів, показано, що зі збільшенням вмісту церію та зростанням температури загальна (χ_{tot}) та ґраткова (χ_{ph}) теплопровідності істотно зменшуються, при цьому густина незначно збільшується (при 300 К). Встановлено залежність теплопровідності від відсоткового вмісту церія. При тривалому відпалі загальна й ґраткова складові теплопровідності зростають. Встановлено, що перенесення тепла в Ce_xSn_{1-x} Se здійснюється переважно фононами.

Ключові слова: тверді розчини, ґраткова теплопровідність, тепловий опір, точкові дефекти, фонон-фононне розсіювання.